JOURNAL OF THERMOPHYSICS AND HEAT TRANSFER
Vol. 14, No. 1, January–March 2000

Transient Coupled Radiation and Conduction in an Absorbing and Scattering Composite Layer

He-Ping Tan,* Ping-Yang Wang,† and Xin-Lin Xia‡
Harbin Institute of Technology, 150001 Harbin, People's Republic of China

A method is developed for obtaining transient temperatures and heat flux densities in a two-layer isotropic scattering semitransparent composite with spectrally dependent radiative properties. The radiative transfer coefficients of the absorbing and isotropic scattering composite are deduced by the ray tracing method in combination with Hottel and Sarofim's zonal method (Hottel, H. C., and Sarofim, A. F., *Radiative Transfer*, McGraw–Hill, New York, 1967, pp. 265, 266). The boundary surfaces and the internal interface are semitransparent, and the reflections are assumed to be diffuse or specular. The radiative heat source term is calculated by the radiative transfer coefficients. The transient energy equation is solved by the full implicit control-volume method in combination with the spectral band model. An advantage of the method is that it needs only to disperse the space position, but not to disperse the solid angle. A comparison of the results, obtained under diffuse reflection, with previous results shows that the equations are correct, and the results are more accurate. The analysis includes the influences of the scattering albedo, the dimensionless thickness, the conduction–radiation parameter, the convection–radiation parameter, the spectral properties, and the reflective mode on the transient temperature field and the heat flux density.

Nomenclature

A_{k,T_i} = fractional spectral emissive power of spectral band k at nodal temperature T_i,

$$\frac{\int_{\Delta\lambda_k} I_{b,\lambda}(T_i)\,\mathrm{d}\lambda}{\int_0^{\infty} I_{b,\lambda}(T_i)\,\mathrm{d}\lambda}$$

$AI1, AI2, \ldots$ = quotient of radiative intensity absorbed by the surface $S_{+\infty}$ (Figs. 3 and 4)
C = unit heat capacity, $\mathrm{J\cdot m^{-3}\cdot K^{-1}}$
C_{21} = dimensionless unit heat capacity, C_2/C_1
$FT, FA,$ FJ, FM = functions for specular or diffuse reflection [Eqs. (7), (A5), and (A6)]
H_1, H_2 = convection–radiation parameter, $h_1/\sigma T_r^3$ and $h_2/\sigma T_r^3$, respectively
h_1, h_2 = convective heat transfer coefficient at surfaces of S_1 and S_2, respectively, $\mathrm{W\cdot m^{-2}\cdot K^{-1}}$
k_{ie}, k_{iw} = harmonic mean thermal conductivity at interfaces ie and iw, $\mathrm{W\cdot m^{-1}\cdot K^{-1}}$
L_b = thickness of each layer in composite, m
L_t = total thickness of composite, $L_1 + L_2$, m
M_b = number of control volumes of each layer
M_t = total number of control volumes of composite, $M_1 + M_2$
N_b = conduction–radiation parameter, $k_b/(4\sigma T_r^3 L_t)$
NB = total number of spectral bands
$n_{b,k}, n_{i,k}$ = spectral refractive index of the bth layer and the ith control volume, respectively, when $i \le M_1 + 1$, $n_{1,k}$; otherwise, $n_{2,k}$
q^{cd}, q^r = thermal conductive and radiative heat fluxes, respectively, $\mathrm{W\cdot m^{-2}}$
$\tilde{q}_{r1}, \tilde{q}_{r2}$ = dimensionless external radiation fluxes incident at $x = 0$ and L_t, $\sigma T_{S_{-\infty}}^4/(\sigma T_r^4)$ and $\sigma T_{S_{+\infty}}^4/(\sigma T_r^4)$, respectively
$\tilde{q}^t$ = dimensionless total heat flux, $(q^{cd} + q^r)/\sigma T_r^4$
S_u, S_0 = black surface, $S_{-\infty}$ or $S_{+\infty}$ and $S_{-\infty}$ or $S_{+\infty}$, respectively
$(S_uS_0)_k, (S_uV_j)_k,$ $(V_iV_j)_k$ = radiation transfer coefficients of surface vs surface, surface vs volume, and volume vs volume in nonscattering media relative to the spectral band $k(\Delta\lambda_k)$
$[S_uS_0]_k, [S_uV_j]_k,$ $[V_iV_j]_k$ = radiation transfer coefficient of surface vs surface, surface vs volume, and volume vs volume in isotropic scattering media relative to the spectral band $k(\Delta\lambda_k)$
S_1, S_2, S_P = boundary surfaces and internal interface (Fig. 1)
$S_{-\infty}, S_{+\infty}$ = black surfaces representing the surroundings
T = absolute temperature, K
T_{g1}, T_{g2} = gas temperatures for convection at $X = 0$ and 1, K
$\tilde{T}_{g1}, \tilde{T}_{g2}$ = dimensionless gas temperatures, T_{g1}/T_r and T_{g2}/T_r, respectively
T_r = reference temperature or uniform initial temperature, K
$T_{S_{-\infty}}, T_{S_{+\infty}}$ = temperatures of the black surfaces $S_{-\infty}$ and $S_{+\infty}$, respectively
$TI1, TI2, \ldots$ = quotient of radiative intensity transmitted (Figs. 3 and 4)
t = physical time, s
t^* = dimensionless time, $(4\sigma T_r^3/C_1L_t)t$
t_s^* = steady-state dimensionless time
x = coordinate in direction across layer, $X = x/L_t$, m
$x_{1_i1_j}, \ldots$ = distance of ray transfer between subscripts, m
z = distance of ray transfer, m
$\alpha_{b,k}$ = spectral absorption coefficient of each layer, $\mathrm{m^{-1}}$
$\gamma_{gb}, \gamma_{bg}, \gamma_{bP}$ = transmissivities at interfaces (Fig. 1)
Δt = time interval, s
Δx = spacing interval between two nodes, m
δ = dimensionless thickness of the first layer L_1/L_t

Received 12 February 1999; revision received 13 July 1999; accepted for publication 13 July 1999.

*Professor, School of Energy Science and Engineering, 92 West Dazhi Street; tanhp@etp4.hit.edu.cn.
†Ph.D. Candidate, School of Energy Science and Engineering, 92 West Dazhi Street; wangpy@263.net.
‡Associate Professor, School of Energy Science and Engineering, 92 West Dazhi Street.

ζ = amount of the control-volume per optical thickness, $\zeta_1 = M_1/\tau_1$, $\zeta_2 = M_2/\tau_2$
η_i = $1 - \omega_i$; when $i \le M_1 + 1$, $\omega_i = \omega_1$; otherwise, $\omega_i = \omega_2$
Θ = dimensionless temperature, T/T_r
θ = angle of reflection or incidence
$\kappa_{b,k}$ = extinction coefficients of each layer, m^{-1}
λ = wavelength, μm
μ = direction cosine, $\cos(\theta)$
$\rho_{gb}, \rho_{bg}, \rho_{bP}$ = reflectivities at interfaces (Fig. 1)
σ = Stefan–Boltzmann constant, $W \cdot m^{-2} \cdot K^{-4}$
$\sigma_{s,k}$ = spectral scattering coefficient, m^{-1}
$\tau_{b,k}$ = spectral optical thickness of each layer
Φ_i^r = radiative heat source of the control-volume i
φ = refractive angle
$\omega_{b,k}$ = spectral single-scattering albedo of each layer, $\sigma_{sb,k}/(\sigma_{sb,k} + \alpha_{b,k})$

Subscripts

a = absorbed quotient in the overall radiative heat transfer coefficient
b = layer index: 1 in first layer, 2 in second layer
c = surface index: 1 or P or 2
h = control-volume index (Appendix)
i, j, l = number of nodes
ie, iw = right and left interface of control volume i (Fig. 1)
k = relative to spectral band k
s = scattered quotient in the overall radiative heat transfer coefficient
$1_i, 2_i$ = ith node in the first and second layers, respectively

Superscripts

d, s = diffuse and specular reflection, respectively
$m, m+1$ = time step

Introduction

THE transient coupled radiative and conductive heat transfer in a semitransparent medium (STM) is one of the pervasive processes in engineering applications, such as tempered glass and the application of its products,[1–3] thermal property analysis for ceramic parts,[4] manufacture and application of optical fiber and its products, processing of multilayer semiconductors, melting and removal of ice layers,[5] transient responses to volumetrically scattering heat shields,[6,7] ignition and flame spread for translucent plastics and solid fuels, and so on.

In the last two decades, some researchers, such as Chan and Cho,[8] Tsai and Nixon,[9] Timoshenko and Trenev,[10] Ho and Özisik,[11] Siegel and Spuckler,[12–14] Spuckler and Siegel,[15] etc., also have focused on coupled heat transfer in a two-layer or multilayer planar STM in addition to the heat transfer in a single layer. Because of the complexity of transient coupled radiative–conductive heat transfer, most of them considered the steady state,[12–15] the same refractive index of the various layers,[8,9] and the gray medium,[8,9,11–13] without considering scattering.[8–10] Siegel[16,17] used the two-flux method in combination with Green's function to study coupled heat transfer in the composite with diffuse interfaces and to obtain steady-state and transient temperature distributions considering the effect of the isotropic scattering and the refractive indexes. Recently, Siegel has reviewed the studies of this subject in detail.[18]

In Ref. 19, the transient coupled radiative and conductive heat transfer in an one-dimensional nongray single-layer STM was investigated by the ray tracing method. In Ref. 19, the radiative properties of various surfaces (opaque or semitransparent boundary surfaces) and thermal boundary conditions are considered. Recently, this method was extended to study transient coupled heat transfer in an isotropic scattering single-layer STM.[20]

The object of this paper is to extend this method to study the transient coupled conduction and radiation in an absorbing and isotropic scattering composite layer. With this aim, the ray tracing method, based on the relations of energy transfer between surface and surface, surface and control volume, and control volume and control volume of Hottel and Sarofim's zonal method,[21] is used to deduce the radiative transfer coefficients (RTCs) of a two-layer isotropic scattering nongray STM with semitransparent boundary surfaces under specular or diffuse reflection. The radiative heat source is obtained by RTCs. The transient energy equation is solved by the control-volume method. The temperature field and the heat flux density distribution in a two-layer planar absorbing and scattering medium are obtained for the general boundary conditions of external convection and radiation.

Physical Model and Governing Equation

Physical Model

The energy equation for transient coupled radiative and conductive heat transfer in a participating medium is given by

$$C\left(\frac{\partial T}{\partial t}\right) = -\mathrm{div}(\boldsymbol{q}^{cd} + \boldsymbol{q}^{r}) \tag{1}$$

The analysis is for an absorbing, emitting, and scattering composite composed of a two-layer planar STM with different optical and thermal properties in different layers. As shown in Fig. 1, the composite is between two black surfaces $S_{-\infty}$ and $S_{+\infty}$ that denote the environment, whose temperatures are $T_{S_{-\infty}}$ and $T_{S_{+\infty}}$, respectively. The boundary surfaces S_1 and S_2 and the internal interface S_P are semitransparent. The first layer is divided into M_1 control volumes along its thickness, and the second layer is divided into M_2 control volumes. Here, $1_i = 1$ and $2_i = M_2 + 1$ are the surfaces S_1 and S_2, respectively. Let $M_t = M_1 + M_2$, then the total number of nodes is $M_t + 2$. For convenience, 1_i and 2_i are shortened to i in the following equations, except for the RTCs. When $i \le M_1 + 1$, i represents the ith node in the first layer and the subscript in the equation $b = 1$; otherwise, i represents the $(i - M_1 - 1)$th node in the second layer and $b = 2$. Therefore, the fully implicit discrete energy equation of the control volume i is obtained as

$$C_b \Delta x (T_i^{m+1} - T_i^m)/\Delta t = \left[k_{ie}^{m+1}(T_{i+1}^{m+1} - T_i^{m+1}) + k_{iw}^{m+1}(T_{i-1}^{m+1} - T_i^{m+1})\right]/\Delta x + \Phi_i^{r,m+1} \quad 2 \le i \le M_t + 1 \tag{2}$$

As shown in Table 1, the radiative properties of STM are simulated by three rectangular spectral bands ($NB = 3$).

Radiative Heat Source

The key to solving the transient discrete energy equation is to solve the local radiative heat source term (Φ_i^r). For the one-dimensional problem, the radiative heat source of the control volume i is equal to the difference of radiative flux densities between its two interfaces[19]:

$$\Phi_i^r = q_{ie}^r(T) - q_{iw}^r(T) = q_{ie}^r(T) - q_{(i-1)e}^r(T) \qquad 2 \le i \le M_t + 1 \tag{3}$$

Table 1 Two spectral band models used for the different semitransparent material

	Model A[a]		Model B[b]	
k	λ, μm	κ_k, m^{-1}	λ, μm	κ_k, m^{-1}
1	0.5–2.7	20	0.5–2.7	2.5
2	2.7–4.5	2,000	2.7–4.5	250
3	4.5–50	10,000	4.5–50	1250

[a] Model A, $n_k = 1.5$, $\omega = 0.5$. [b] Model B, $n_k = 3.0$, $\omega = 0$.

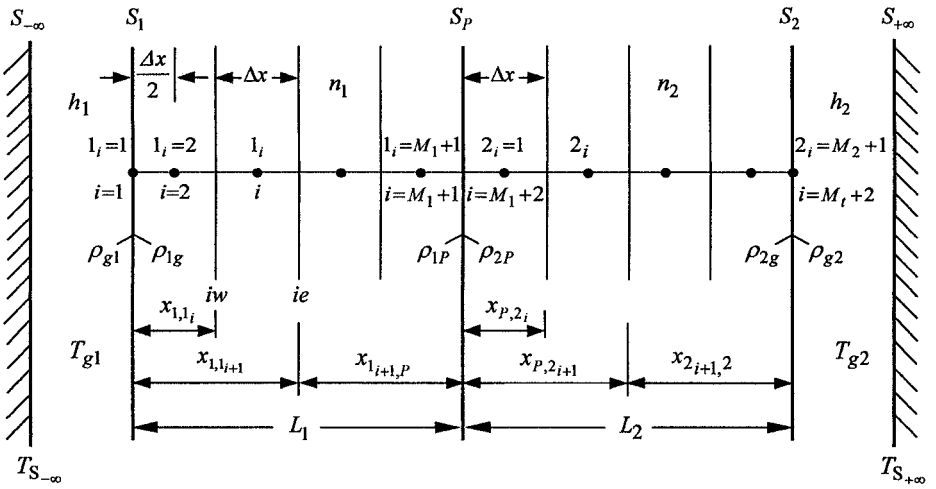

Fig. 1 Zonal discretion model of two-layer planar composite.

When the boundary surfaces S_1 and S_2 are semitransparent, q^r_{ie} can be expressed as

$$q^r_{ie} = \sigma \sum_{k=1}^{NB} \left\{ \sum_{j=2}^{i} ([S_{+\infty} V_j]_k A_{k,T_{S_{+\infty}}} T^4_{S_{+\infty}} - n^2_{j,k}[V_j S_{+\infty}]_k A_{k,T_j} T^4_j) + \sum_{j=i+1}^{M_t+1} \sum_{l=2}^{i} (n^2_{j,k}[V_j V_l]_k A_{k,T_j} T^4_j - n^2_{l,k}[V_l V_j]_k A_{k,T_l} T^4_l) + \sum_{j=i+1}^{M_t+1} (n^2_{j,k}[V_j S_{-\infty}]_k A_{k,T_j} T^4_j - [S_{-\infty} V_j]_k A_{k,T_{S_{-\infty}}} T^4_{S_{-\infty}}) + [S_{+\infty} S_{-\infty}]_k A_{k,T_{S_{+\infty}}} T^4_{S_{+\infty}} - [S_{-\infty} S_{+\infty}]_k A_{k,T_{S_{-\infty}}} T^4_{S_{-\infty}} \right\} \quad (4)$$

The radiative heat source can be rewritten as

$$\Phi^r_i = \sigma \sum_{k=1}^{NB} \left\{ ([S_{+\infty} V_i]_k A_{k,T_{S_{+\infty}}} T^4_{S_{+\infty}} - n^2_{i,k}[V_i S_{+\infty}]_k A_{k,T_i} T^4_i) + \sum_{j=2}^{M_t+1} (n^2_{j,k}[V_j V_i]_k A_{k,T_j} T^4_j - n^2_{i,k}[V_i V_j]_k A_{k,T_i} T^4_i) + ([S_{-\infty} V_i]_k A_{k,T_{S_{-\infty}}} T^4_{S_{-\infty}} - n^2_{i,k}[V_i S_{-\infty}]_k A_{k,T_i} T^4_i) \right\}$$

$$2 \le i \le M_t + 1 \quad (5)$$

where when $i,\ j \le M_1 + 1$, $n_i = n_1$, and $n_j = n_1$; otherwise, $n_i = n_2$ and $n_j = n_2$.

When $i = 1$ and $M_t + 2$, the radiative heat flux at the boundary surfaces $q^r_{S_1}$ and $q^r_{S_2}$ are

$$q^r_{S_1} = q^r_{1w} = \sigma \sum_{k=1}^{NB} \left\{ \sum_{j=2}^{M_t+1} (n^2_{j,k}[V_j S_{-\infty}]_k A_{k,T_j} T^4_j - [S_{-\infty} V_j]_k A_{k,T_{S_{-\infty}}} T^4_{S_{-\infty}}) + [S_{+\infty} S_{-\infty}]_k A_{k,T_{S_{+\infty}}} T^4_{S_{+\infty}} - [S_{-\infty} S_{+\infty}]_k A_{k,T_{S_{-\infty}}} T^4_{S_{-\infty}} \right\} \quad (6a)$$

$$q^r_{S_2} = q^r_{(M_t+1)e} = \sigma \sum_{k=1}^{NB} \left\{ \sum_{j=2}^{M_t+1} ([S_{+\infty} V_j]_k A_{k,T_{S_{+\infty}}} T^4_{S_{+\infty}} - n^2_{j,k}[V_j S_{+\infty}]_k A_{k,T_j} T^4_j) + [S_{+\infty} S_{-\infty}]_k A_{k,T_{S_{+\infty}}} T^4_{S_{+\infty}} - [S_{-\infty} S_{+\infty}]_k A_{k,T_{S_{-\infty}}} T^4_{S_{-\infty}} \right\} \quad (6b)$$

From the foregoing process, we can see the difficulty in solving the radiative heat source and the radiative heat flux density is in calculating the RTCs.

RTC of a Two-Layer Composite

The RTC of a surface or a control-volume element i vs element j is defined as the quotient of the radiative energy absorbed by element j in the transfer process of the radiative energy emitted by element i. For the scattering STM, the transfer process includes 1) the radiative energy directly reaching element j, 2) the reflection by surfaces once or many times, and 3) the scattering by the medium once or many times.

Though the transfer of radiative energy is completed instantly, the transfer process can be divided into two subprocesses according to the transfer mechanism of radiative energy in the STM.

1) Only the absorption and emission of the medium are considered, that is, the radiative energy emitted by element i directly or after surface reflections reaches element j. For this condition, the RTC is presented by $(S_u S_0)$, $(S_u V_j)$, and $(V_i V_j)$.

2) When scattering is considered, the quotient of the radiative energy represented by the RTCs for the absorbing, emitting medium should be redistributed. After scattering once, a part of radiative energy represented by the RTC is absorbed by the STM, and the rest is scattered. For isotropic scattering, the radiative intensity scattered by element j is distributed uniformly. Such a distribution is equivalent to the distribution of the radiative intensity emitted by element j. When the effect of scattering is considered, the RTC is presented by $[S_u S_0]$, $[S_u V_j]$, and $[V_i V_j]$.

In this paper, RTCs without a superscript may be applied to either specular or diffuse reflection. For convenience, subscript k of the variables denoting spectral properties ρ, γ, and ω is omitted in the deductive process in the text.

RTC for an Absorbing, Emitting Composite Under Specular Reflection

Under specular reflection, the incident angle of the ray (denoting the radiative intensity) is equal to the reflective angle, as shown in Fig. 2; therefore, two rays with different launching angles cannot intersect. Thus, the attenuation function of the radiative intensity with an arbitrary launching angle along the transferring path can be

found by tracing this ray; then the RTC, taking into consideration reflections for an absorbing, emitting STM, can be calculated by integrating in hemisphere space.

Briefly, four functions are defined.

1) The transmissivity after the radiative intensity transferring through the distance z/μ_b in the bth layer:

$$FT_{b,k}(z) = \exp(-\kappa_{b,k} z/\mu_b) \tag{7a}$$

2) In the transfer process of the radiative intensity in the single-layer (bth layer) STM, the total radiative intensity reaching a certain element is the sum of a geometric progression, as shown in Fig. 3. Assume $FJ_{b,k}$ to be the common ratio of the geometric progression and to be given by

$$FJ_{b,k} = \rho_{bP}\rho_{bg} FT_{b,k}(2L_b) \tag{7b}$$

3) In the radiative intensity transfer process in the two-layer STM, the total radiative intensity reaching a certain element is also the sum of a geometric progression, as shown in Figs. 3 and 4. Assume FJ_k to be the common ratio of the geometric progression and to be given by

$$FJ_k = \frac{\gamma_{1P}\gamma_{2P}\rho_{1g}\rho_{2g} FT_{1,k}(2L_1) FT_{2,k}(2L_2)}{(1 - FJ_{1,k})\cdot(1 - FJ_{2,k})} \tag{7c}$$

4) From the energy transferring relations of the zonal method[21] and the geometric relations in Fig. 1,

$$(S_i V_j) = (S_i S_j) - (S_i S_{j+1}), \qquad x_{i,j+1} = x_{i,j} + \Delta x$$

we can obtain the radiative intensity factor of the emission and absorption by some element in the bth layer:

$$FA_{b,k} = 1 - FT_{b,k}(\Delta x) \tag{7d}$$

By reference to Figs. 3 and 4, the process of deducing RTC $(S_{-\infty} S_{+\infty})_k^s$ is provided. After passing through surface S_1, the radiative intensity emitted by the black surface $S_{-\infty}$ at a certain angle enters the first layer, where it is attenuated to zero due to multiple reflection, transmission, and absorption. In this process, a part of radiative intensity enters the second layer and is denoted $TI1$. $TI1$ can be divided into three parts.

1) The first part is absorbed by the second layer.

2) The second part reaches the black surface $S_{+\infty}$ through the surface S_2 and is denoted $AI1$.

3) The last part, denoted $TI2$, goes back to the first layer through the surface S_P. A part of $TI2$ transmits into the second layer again through the surface S_P in the transferring process in the first layer and is denoted $TI3$. $TI3$ carries out the foregoing process repeatedly, and a part of it, denoted $AI2$, can reach the black surface $S_{+\infty}$ again.

The described process is carried out repeatedly (see Fig. 4) until the radiative intensity emitted by the black surface $S_{-\infty}$ and transmitted into the composite is attenuated to zero. In Fig. 4, every beeline with arrowhead and every flexline with arrowhead within each layer denotes a process in Fig. 3; the radiative intensity is repeatedly attenuated to zero in the process of reflection, absorption, and transmission in that layer. In this process, the beeline and flexline within each layer denote the attenuation factors $FT_{b,k}(L_b)/(1 - FJ_{b,k})$ and $FT_{b,k}(2L_b)/(1 - FJ_{b,k})$, respectively. After being transmitted once, the radiative intensity emitted by the surface $S_{-\infty}$ and absorbed by the surface $S_{+\infty}$ is called the first-order absorption and is denoted by the superscript 1st:

$$(S_{-\infty} S_{+\infty})_k^{s,1\text{st}} = AI1 = \gamma_{g1}\cdot\frac{FT_{1,k}(L_1)}{1 - FJ_{1,k}}\cdot\gamma_{1P}\frac{FT_{2,k}(L_2)}{1 - FJ_{2,k}}\cdot\gamma_{2g} \tag{8}$$

The second-order absorption is

$$(S_{-\infty} S_{+\infty})_k^{s,2\text{nd}} = AI2$$

$$= \frac{\gamma_{g1}\cdot\gamma_{1P}\cdot\gamma_{2g}\cdot FT_{1,k}(L_1)\cdot FT_{2,k}(L_2)}{(1 - FJ_{1,k})\cdot(1 - FJ_{2,k})}$$

$$\times\left[\frac{\rho_{1g}\gamma_{1P} FT_{1,k}(2L_1)}{1 - FJ_{1,k}}\cdot\frac{\rho_{2g}\gamma_{2P} FT_{2,k}(2L_2)}{1 - FJ_{2,k}}\right]^1 \tag{9}$$

The third-order absorption is

$$(S_{-\infty} S_{+\infty})_k^{s,3\text{rd}} = \frac{\gamma_{g1}\cdot\gamma_{1P}\cdot\gamma_{2g}\cdot FT_{1,k}(L_1)\cdot FT_{2,k}(L_2)}{(1 - FJ_{1,k})\cdot(1 - FJ_{2,k})}$$

$$\times\left[\frac{\rho_{1g}\gamma_{1P} FT_{1,k}(2L_1)}{1 - FJ_{1,k}}\cdot\frac{\rho_{2g}\gamma_{2P} FT_{2,k}(2L_2)}{1 - FJ_{2,k}}\right]^2 \tag{10}$$

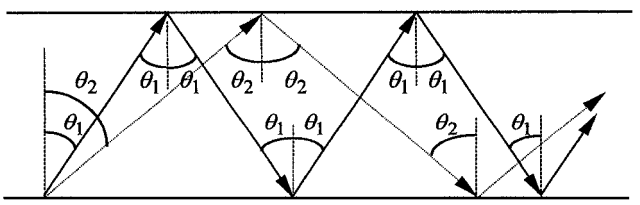

Fig. 2 Two rays tracing with launching angle θ_1 and θ_2 under specular reflection.

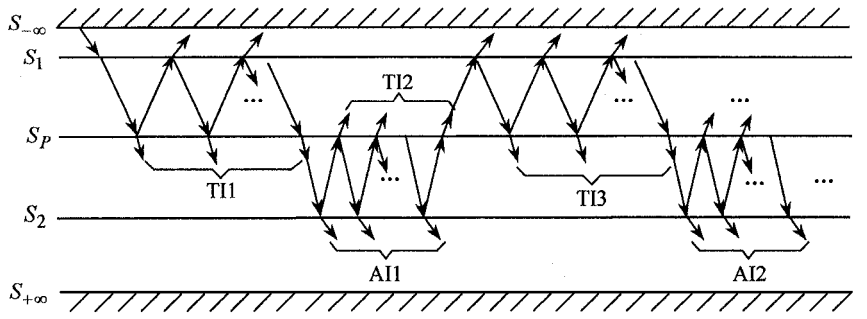

Fig. 3 Diagram of the radiative intensity transferring in a two-layer STM under specular reflection.

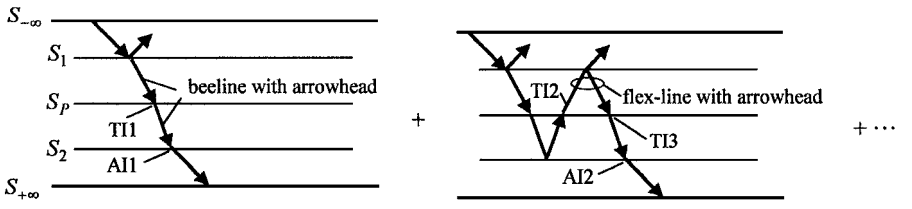

First-order absorption **Second-order absorption**

Fig. 4 Diagram of the radiative intensity equivalent transferring in the composite.

The $(n+1)$th-order absorption is

$$(S_{-\infty}S_{+\infty})_k^{s,(n+1)\text{th}} = \frac{\gamma_{g1}\cdot\gamma_{1P}\cdot\gamma_{2g}\cdot FT_{1,k}(L_1)\cdot FT_{2,k}(L_2)}{(1-FJ_{1,k})\cdot(1-FJ_{2,k})} \times\left[\frac{\rho_{1g}\gamma_{1P}FT_{1,k}(2L_1)}{1-FJ_{1,k}}\cdot\frac{\rho_{2g}\gamma_{2P}FT_{2,k}(2L_2)}{1-FJ_{2,k}}\right]^n \tag{11}$$

According to the preceding analysis, in the entire transfer process, that is, the attenuation to zero of the radiative intensity emitted by $S_{-\infty}$ and transmitted into the composite, the total radiative intensity absorbed by the black surface $S_{+\infty}$ is the sum of the geometric progression. Then $(S_{-\infty}S_{+\infty})_k^s$ can be calculated by integrating the total radiative intensity in hemisphere space,

$$\begin{aligned}(S_{-\infty}S_{+\infty})_k^s &= 2\int_0^1 \left[(S_{-\infty}S_{+\infty})_k^{s,1\text{st}} + (S_{-\infty}S_{+\infty})_k^{s,2\text{nd}} + (S_{-\infty}S_{+\infty})_k^{s,3\text{rd}} + \cdots\right]\mu_1\,\mathrm{d}\mu_1 \\ &= 2\int_0^1 \frac{\gamma_{g1}\cdot\gamma_{1P}\cdot\gamma_{2g}\cdot FT_{1,k}(L_1)\cdot FT_{2,k}(L_2)}{(1-FJ_{1,k})\cdot(1-FJ_{2,k})\cdot(1-FJ_k)}\mu_1\,\mathrm{d}\mu_1\end{aligned} \tag{12}$$

For a two-layer STM, there are 18 RTCs: 16 of them are used in calculating the temperature field; the others are the self-RTCs and are used in calculating the integrality of the RTCs. For the relativity of the RTC, the 16 RTCs can be sorted into 8 pairs:

$$\begin{aligned}(S_{-\infty}S_{+\infty})_k^s &= (S_{+\infty}S_{-\infty})_k^s, & (S_{-\infty}V_{1_j})_k^s &= n_{1,k}^2(V_{1_j}S_{-\infty})_k^s \\ (S_{-\infty}V_{2_j})_k^s &= n_{2,k}^2(V_{2_j}S_{-\infty})_k^s, & (S_{+\infty}V_{1_j})_k^s &= n_{1,k}^2(V_{1_j}S_{+\infty})_k^s \\ (S_{+\infty}V_{2_j})_k^s &= n_{2,k}^2(V_{2_j}S_{+\infty})_k^s, & n_{1,k}^2(V_{1_i}V_{2_j})_k^s &= n_{2,k}^2(V_{2_j}V_{1_i})_k^s \\ (V_{1_i}V_{1_j})_k^s &= (V_{1_j}V_{1_i})_k^s, & (V_{2_i}V_{2_j})_k^s &= (V_{2_j}V_{2_i})_k^s\end{aligned} \tag{13}$$

To obtain other RTCs, the processes are similar to that of $(S_{-\infty}S_{+\infty})_k^s$:

$$(S_{-\infty}V_{1_j})_k^s = 2\gamma_{g1}n_{1,k}^2\int_{\mu_{1g}}^1 FA_{1,k}\left\{\frac{FT_{1,k}(x_{1,1_j}) + \rho_{1P}FT_{1,k}(L_1+x_{P,1_{j+1}})}{1-FJ_{1,k}} + \frac{\gamma_{1P}\gamma_{2P}\rho_{2g}FT_{1,k}(L_1)FT_{2,k}(2L_2)\left[FT_{1,k}(x_{P,1_{j+1}}) + \rho_{1g}FT_{1,k}(L_1+x_{1,1_j})\right]}{(1-FJ_{1,k})^2\cdot(1-FJ_{2,k})\cdot(1-FJ_k)}\right\}\mu_1\,\mathrm{d}\mu_1 \tag{14}$$

$$(S_{-\infty}V_{2_j})_k^s = 2\gamma_{g1}n_{2,k}^2\int_{\mu_{2g}}^1 FA_{2,k}\frac{\gamma_{1P}FT_{1,k}(L_1)\cdot\left[FT_{2,k}(x_{P,2_j}) + \rho_{2g}FT_{2,k}(L_2+x_{2,2_{j+1}})\right]}{(1-FJ_{1,k})\cdot(1-FJ_{2,k})\cdot(1-FJ_k)}\mu_2\,\mathrm{d}\mu_2 \tag{15}$$

$$(S_{+\infty}V_{1_j})_k^s = 2\gamma_{g2}n_{1,k}^2\int_{\mu_{1g}}^1 FA_{1,k}\frac{\gamma_{2P}FT_{2,k}(L_2)\left[FT_{1,k}(x_{P,1_{j+1}}) + \rho_{1g}FT_{1,k}(L_1+x_{1,1_j})\right]}{(1-FJ_{1,k})\cdot(1-FJ_{2,k})\cdot(1-FJ_k)}\mu_1\,\mathrm{d}\mu_1 \tag{16}$$

$$(S_{+\infty}V_{2_j})_k^s = 2\gamma_{g2}n_{2,k}^2\int_{\mu_{2g}}^1 FA_{2,k}\left\{\frac{FT_{2,k}(x_{2,2_{j+1}}) + \rho_{2P}FT_{2,k}(L_2+x_{P,2_j})}{1-FJ_{2,k}} + \frac{\gamma_{1P}\gamma_{2P}\rho_{1g}FT_{2,k}(L_2)FT_{1,k}(2L_1)\left[FT_{2,k}(x_{P,2_j}) + \rho_{2g}FT_{2,k}(L_2+x_{2,2_{j+1}})\right]}{(1-FJ_{1,k})\cdot(1-FJ_{2,k})^2\cdot(1-FJ_k)}\right\}\mu_2\,\mathrm{d}\mu_2 \tag{17}$$

$$(V_{1_i}V_{2_j})_k^s = 2\int_{\mu_{21}}^1 \frac{\left[\rho_{1g}FT_{1,k}(x_{1_i,1}+L_1) + FT_{1,k}(x_{1_{i+1},P})\right]\left[FT_{2,k}(x_{P,2_j}) + \rho_{2g}FT_{2,k}(L_2+x_{2,2_{j+1}})\right]}{n_{1,k}^2(1-FJ_{1,k})\cdot(1-FJ_{2,k})\cdot(1-FJ_k)/\left[n_{2,k}^2\gamma_{1P}FA_{1,k}FA_{2,k}\right]}\mu_2\,\mathrm{d}\mu_2 \tag{18}$$

$$(V_{1_i}V_{1_j})_k^s = R_{1,k} + 2\int_0^1 \frac{FA_{1,k}^2}{1-FJ_{1,k}}\left\{\rho_{1_g}FT_{1,k}(x_{1_i,1}+x_{1,1_j}) + \rho_{1g}\rho_{1P}FT_{1,k}(x_{1_i,1}+L_1+x_{P,1_{j+1}}) + \rho_{1P}FT_{1,k}(x_{1_{i+1},P}+x_{P,1_{j+1}}) + \rho_{1g}\rho_{1P}FT_{1,k}(x_{1_{i+1},P}+L_1+x_{1,1_j}) + \frac{\left[\rho_{1g}FT_{1,k}(x_{1_i,1}+L_1) + FT_{1,k}(x_{1_{i+1},P})\right]\left[FT_{1,k}(x_{P,1_{j+1}}) + \rho_{1g}FT_{1,k}(L_1+x_{1,1_j})\right]}{(1-FJ_{1,k})\cdot(1-FJ_{2,k})\cdot(1-FJ_k)/[\rho_{2g}\gamma_{1P}\gamma_{2P}FT_{2,k}(2L_2)]}\right\}\mu_1\,\mathrm{d}\mu_1 \tag{19}$$

$$(V_{2_i}V_{2_j})_k^s = R_{2,k} + 2\int_0^1 \frac{FA_{2,k}^2}{1-FJ_{2,k}}\left\{\rho_{2P}FT_{2,k}(x_{2_i,P}+x_{P,2_j}) + \rho_{2g}\rho_{2P}FT_{2,k}(x_{2_{i+1},2}+L_2+x_{P,2_j}) + \rho_{2g}\rho_{2P}FT_{2,k}(x_{2_i,P}+L_2+x_{2,2_{j+1}}) + \rho_{2g}FT_{1,k}(x_{2_{i+1},2}+x_{2,2_{j+1}}) + \frac{\left[FT_{2,k}(x_{2_i,P}) + \rho_{2g}FT_{2,k}(x_{2_{i+1},2}+L_2)\right]\left[FT_{2,k}(x_{P,2_j}) + \rho_{2g}FT_{2,k}(L_2+x_{2,2_{j+1}})\right]}{(1-FJ_{1,k})\cdot(1-FJ_{2,k})\cdot(1-FJ_k)/[\rho_{1g}\gamma_{2P}\gamma_{1P}FT_{1,k}(2L_1)]}\right\}\mu_2\,\mathrm{d}\mu_2 \tag{20}$$

The self-RTCs of the black surfaces $S_{-\infty}$ and $S_{+\infty}$ are

$$(S_{-\infty}S_{-\infty})_k^s = \rho_{g1} + 2\gamma_{g1}\gamma_{1g}n_{1,k}^2\int_{\mu_{1g}}^1\left\{\frac{\rho_{1P}FT_{1,k}(2L_1)}{1-FJ_{1,k}} + \frac{\gamma_{1P}\gamma_{2P}\rho_{2g}FT_{1,k}(2L_1)FT_{2,k}(2L_2)}{(1-FJ_{1,k})^2\cdot(1-FJ_{2,k})\cdot(1-FJ_k)}\right\}\mu_1\,\mathrm{d}\mu_1 \tag{21}$$

$$(S_{+\infty}S_{+\infty})_k^s = \rho_{g2} + 2\gamma_{g2}\gamma_{2g}n_{2,k}^2\int_{\mu_{2g}}^1\left\{\frac{\rho_{2P}FT_{2,k}(2L_2)}{1-FJ_{2,k}} + \frac{\gamma_{2P}\gamma_{1P}\rho_{1g}FT_{2,k}(2L_2)FT_{1,k}(2L_1)}{(1-FJ_{1,k})\cdot(1-FJ_{2,k})^2\cdot(1-FJ_k)}\right\}\mu_2\,\mathrm{d}\mu_2 \tag{22}$$

where μ_{1g}, μ_{2g}, and μ_{21} are the critical direction cosines, $\mu_{1g} = \sqrt{[1 - (1/n_{1,k}^2)]}$, $\mu_{2g} = \sqrt{[1 - (1/n_{2,k}^2)]}$, and $\mu_{21} = \sqrt{[1 - (n_{1,k}^2/n_{2,k}^2)]}$. When $i \neq j$,

$$R_{b,k} = 2\int_0^1 FA_{b,k}^2 \cdot FT_{b,k}(x_{b_i,b_j})\mu_b \, \mathrm{d}\mu_b$$

When $i = j$,

$$R_{b,k} = 4\kappa_{b,k}\Delta x - 2[1 - 2E_3(\kappa_{b,k}\Delta x)]$$

A limit condition, $n_{1,k} \leq n_{2,k}$, is implied in these equations. Thus, the following limit conditions must be met: if $0 \leq \mu_1 \leq \mu_{1g}$, then $\rho_{1g} = \rho_{2g} = 1$ and $\gamma_{2P} = 0$; if $0 \leq \mu_2 \leq \mu_{21}$, then $\rho_{2P} = \rho_{2g} = 1$; if $\mu_{21} < \mu_2 \leq \mu_{2g}$, then $\rho_{2g} = \rho_{1g} = 1$.

RTC for an Absorbing, Emitting Composite Under Diffuse Reflection

Under specular reflection, the radiative intensity is traced when the RTC is obtained by the ray tracing method; whereas under diffuse reflection, the radiative energy is traced. However, the tracing process of the ray is the same, and so it is omitted here. The RTC and its relativity under diffuse reflection are provided in the Appendix.

RTC of an Absorbing, Emitting, Isotropic Scattering Composite

When the effect of scattering is considered, the quotient of radiative energy represented by RTCs $(S_u S_0)$, $(S_u V_j)$, and $(V_i V_j)$ will be redistributed. For the convenience, subscript k and superscripts s or d are omitted in the following equations. This is because, when isotropic scattering is considered, the deductive process and the ultimate form of the RTC equation is the same regardless if it is spectral or gray, specular or diffuse. The RTC for the single-layer absorbing, emitting, and isotropic scattering STM is seen in Ref. 20. In the following equations, the subscripts a and s are the absorption and scattering quotient in the RTC, respectively.

The effect of the surface reflection has been considered in RTCs $(S_u S_0)$, $(S_u V_j)$, and $(V_i V_j)$. The effect of isotropic scattering will be considered in the following analysis. The process of deducing RTC, considering isotropic scattering, is given here using $[V_i V_j]$ as an example. After the first-order scattering, in the quotient of the energy transfer denoted by the RTC $(V_i V_j)$, only η_j is absorbed, that is, $[V_i V_j]_a^{1\text{st}} = (V_i V_j) \times \eta_j$. After the second-order scattering,

$$[V_i V_j]_a^{2\text{nd}} = [V_i V_j]_a^{1\text{st}} + \sum_{l_2=2}^{M_t+1} (V_i V_{l_2})\omega_{l_2} \times (V_{l_2} V_j)\eta_j$$

After the third-order scattering,

$$[V_i V_j]_a^{3\text{rd}} = [V_i V_j]_a^{2\text{nd}} + \sum_{l_2=2}^{M_t+1} (V_i V_{l_2})\omega_{l_2} \times \left[\sum_{l_3=2}^{M_t+1} (V_{l_2} V_{l_3})\omega_{l_3} \times (V_{l_3} V_j)\eta_j\right]$$

After the fourth-order scattering,

$$[V_i V_j]_a^{4\text{th}} = [V_i V_j]_a^{3\text{rd}} + \sum_{l_2=2}^{M_t+1} (V_i V_{l_2})\omega_{l_2} \times \left\{\sum_{l_3=2}^{M_t+1} (V_{l_2} V_{l_3})\omega_{l_3} \times \left[\sum_{l_4=2}^{M_t+1} (V_{l_3} V_{l_4})\omega_{l_4} \times (V_{l_4} V_j)\eta_j\right]\right\}$$

The rest are deduced by analogy. After the $(n+1)$th-order scattering, each RTC is given by

$$[V_i V_j]_a^{(n+1)\text{th}} = [V_i V_j]_a^{n\text{th}} + \sum_{l_2=2}^{M_t+1} (V_i V_{l_2})\omega_{l_2} \times \left(\sum_{l_3=2}^{M_t+1} (V_{l_2} V_{l_3})\omega_{l_3} \times \left\{\sum_{l_4=2}^{M_t+1} (V_{l_3} V_{l_4})\omega_{l_4} \times \cdots \times \left[\sum_{l_{n+1}=2}^{M_t+1} (V_{l_n} V_{l_{n+1}})\omega_{l_{n+1}} \times (V_{l_{n+1}} V_j)\eta_j\right]\right\}\right) \tag{23a}$$

$$[V_i S_0]_a^{(n+1)\text{th}} = [V_i S_0]_a^{n\text{th}} + \sum_{l_2=2}^{M_t+1} (V_i V_{l_2})\omega_{l_2} \times \left(\sum_{l_3=2}^{M_t+1} (V_{l_2} V_{l_3})\omega_{l_3} \times \left\{\sum_{l_4=2}^{M_t+1} (V_{l_3} V_{l_4})\omega_{l_4} \times \cdots \times \left[\sum_{l_{n+1}=2}^{M_t+1} (V_{l_n} V_{l_{n+1}})\omega_{l_{n+1}} \times (V_{l_{n+1}} S_0)\right]\right\}\right) \tag{23b}$$

$$[S_u V_j]_a^{(n+1)\text{th}} = [S_u V_j]_a^{n\text{th}} + \sum_{l_2=2}^{M_t+1} (S_u V_{l_2})\omega_{l_2} \times \left(\sum_{l_3=2}^{M_t+1} (V_{l_2} V_{l_3})\omega_{l_3} \times \left\{\sum_{l_4=2}^{M_t+1} (V_{l_3} V_{l_4})\omega_{l_4} \times \cdots \times \left[\sum_{l_{n+1}=2}^{M_t+1} (V_{l_n} V_{l_{n+1}})\omega_{l_{n+1}} \times (V_{l_{n+1}} V_j)\eta_j\right]\right\}\right) \tag{23c}$$

$$[S_u S_0]_a^{(n+1)\text{th}} = [S_u S_0]_a^{n\text{th}} + \sum_{l_2=2}^{M_t+1} (S_u V_{l_2})\omega_{l_2} \times \left(\sum_{l_3=2}^{M_t+1} (V_{l_2} V_{l_3})\omega_{l_3} \times \left\{\sum_{l_4=2}^{M_t+1} (V_{l_3} V_{l_4})\omega_{l_4} \times \cdots \times \left[\sum_{l_{n+1}=2}^{M_t+1} (V_{l_n} V_{l_{n+1}})\omega_{l_{n+1}} \times (V_{l_{n+1}} S_0)\right]\right\}\right) \tag{23d}$$

$$[V_i V_j]_s^{(n+1)\text{th}} = \sum_{l_2=2}^{M_t+1} (V_i V_{l_2})\omega_{l_2} \times \left(\sum_{l_3=2}^{M_t+1} (V_{l_2} V_{l_3})\omega_{l_3} \times \left\{\sum_{l_4=2}^{M_t+1} (V_{l_3} V_{l_4})\omega_{l_4} \times \cdots \times \left[\sum_{l_{n+1}=2}^{M_t+1} (V_{l_n} V_{l_{n+1}})\omega_{l_{n+1}} \times (V_{l_{n+1}} V_j)\omega_j\right]\right\}\right) \tag{23e}$$

$$[S_u V_j]_s^{(n+1)\text{th}} = \sum_{l_2=2}^{M_t+1} (S_u V_{l_2})\omega_{l_2} \times \left(\sum_{l_3=2}^{M_t+1} (V_{l_2} V_{l_3})\omega_{l_3} \times \left\{\sum_{l_4=2}^{M_t+1} (V_{l_3} V_{l_4})\omega_{l_4} \times \cdots \times \left[\sum_{l_{n+1}=2}^{M_t+1} (V_{l_n} V_{l_{n+1}})\omega_{l_{n+1}} \times (V_{l_{n+1}} V_j)\omega_j\right]\right\}\right) \tag{23f}$$

Determination of Reflectivity

It is assumed that each bit of roughness acts as a smooth facet so that the reflectivities under diffuse reflection are also determined from n_b using Fresnel equations.[13] When the electromagnetic wave within the spectra band k incidents on the medium with the spectra refractive index $n_{2,k}$ from the medium with the refractive index $n_{1,k}$ at the incidence angle θ, the refractive angle is $\varphi = \arcsin[n_{1,k}\sin(\theta)/n_{2,k}]$. The spectra reflectivity ρ_k is given as

$$\rho_k = \int_0^{\pi/2} \left\{ \left[\frac{n_{2,k}\cos(\varphi) - n_{1,k}\cos(\theta)}{n_{2,k}\cos(\varphi) + n_{1,k}\cos(\theta)} \right]^2 + \left[\frac{n_{1,k}\cos(\varphi) - n_{2,k}\cos(\theta)}{n_{1,k}\cos(\varphi) + n_{2,k}\cos(\theta)} \right]^2 \right\} \sin(\theta)\cos(\theta)\,\mathrm{d}\theta \qquad (24)$$

Under specular reflection, the RTC was deduced here considering the effect of the total reflection. Therefore, when the ray projects into a medium with a smaller refractive index, the reflectivity is obtained from Eq. (24) with the condition that the ray projects from the inverse direction. For the diffuse surface, the effect of the total reflection is considered in the reflectivity, so that the reflectivity is directly calculated from Eq. (24) regardless of the rays' projection side.

Results and Analysis

Temperature Distributions Comparison with Refs. 15 and 16

Under diffuse reflection, Fig. 5 provides a comparison with an exact numerical solution[15] and an approximate solution using Green's function and the two-flux method.[16] Figure 5a has results for the same parameters as Fig. 5b except that the scattering albedo of the first layer is different. The parameters are $n_1 = 1.5$, $n_2 = 3$, $\tau_1 = \tau_2 = 1$ $\tilde{q}_{r1} = 1.0^4$, $\tilde{q}_{r2} = 0.25^4$, $N_1 = N_2 = 0.0625$, $H_1 = H_2 = 1$, $\tilde{T}_{g1} = 1$, $\tilde{T}_{g2} = 0.25$, $\delta = 0.5$, and $C_{21} = 1$. As shown in Fig. 5, the results of this paper are almost the same as the exact numerical solution in Ref. 15, so that it is difficult to distinguish both the curves without scattering and with scattering, whereas

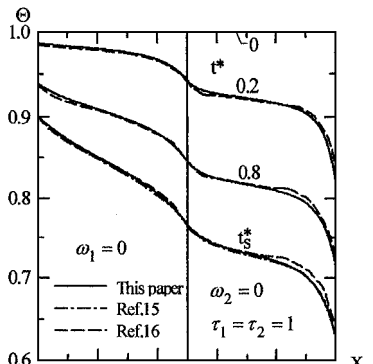

a) Without scattering in both layers

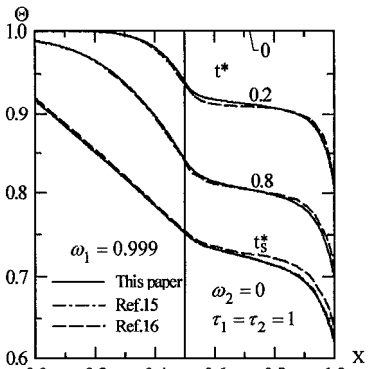

b) Isotropic scattering in the first layer

Fig. 5 Comparison of temperature distributions obtained here with Refs. 15 and 16.

Table 2 Comparison of the dimensionless radiative heat fluxes obtained here with those of Ref. 12 ($\zeta_1 = \zeta_2 = \zeta$)

n_1	n_2	τ_1	τ_2	$\tilde{q}^r_{12}$ (Ref. 12)	ζ	$\tilde{q}^r_{12}$ (this paper)
1	1	20	20	0.0323	5	0.0324283
1	1	20	20	0.0323	7	0.0322801
1	1	20	20	0.0323	10	0.0322001
1	1	20	20	0.0323	20	0.0321417
1	1	20	20	0.0323	30	0.0321307
1	3	20	20	0.0518	5	0.0520065
1	3	20	20	0.0518	7	0.0517946
1	3	20	20	0.0518	10	0.0516802
1	3	20	20	0.0518	20	0.0515966
1	3	20	20	0.0518	30	0.0515810
1.5	3	10	3	0.1656	10	0.1648266
1.5	3	10	3	0.1656	20	0.1646371
1.5	3	1	3	0.3290	10	0.3256801
1.5	3	1	3	0.3290	20	0.3255237
2	4	1	0.1	0.3393	10	0.3375777
2	4	1	0.1	0.3393	20	0.3375142

the approximate results in Ref. 16 deviate a little from the results in Ref. 15. This demonstrates that the equations obtained here are correct, and the accuracy of the method developed is high because the space solid angle is not dispersed but is directly integrated.

Heat Flux Densities Comparison with Ref. 12

Under the steady-state condition, neglecting heat conduction and diffuse reflection, the dimensionless radiative heat flux density, $\tilde{q}^r_{12} = q^r_{12}/(\sigma T^4_{S_{-\infty}} - \sigma T^4_{S_{+\infty}})$, in the two-layer semitransparent media is calculated in Ref. 12 (where $T_{S_{-\infty}} > T_{S_{+\infty}}$; the subscript 12 denotes that $\tilde{q}^r_{12}$ is defined by Ref. 12). From Table 1 in Ref. 12, it can be seen that the diffuse approximation results (the dimensionless temperature distribution Φ and dimensionless radiative heat flux Ψ) are accurate to at least the second decimal place as compared with the exact results when the optical thickness is equal to 10 and 100. However, only the first decimal place is assured when the optical thickness is equal to 0.1 and 1. Comparison of the results in this paper with those in Ref. 12 for the case $\zeta_1 = \zeta_2 = \zeta = 5 \sim 30$ is shown in Table 2. We can see the following. 1) When $\tau_1 = \tau_2 = 20$, the results in this paper well agree with those in Ref. 12, but with the decrease of the optical thickness, a deviation appears. 2) With the increase of ζ, the deviation is larger and approaches a constant. Take the case of $\tau_1 = \tau_2 = 20$ as an example: When $\zeta = 7$, the results in this paper are the same as those in Ref. 12, but further increase of ζ will cause the deviation.

Effect of the Scattering Albedo on Temperature Distributions

Figure 6 shows the effect of scattering albedo ω_1 of the first layer on the temperature distributions in the composite for the case $n_1 = 1.5$, $n_2 = 3.0$, $\tilde{q}_{r1} = 1.5^4$, $\tilde{q}_{r2} = 0.5^4$, $N_1 = N_2 = 0.025$, $H_1 = H_2 = 5$, $\tilde{T}_{g1} = \tilde{T}_{g2} = 1$, $\delta = 0.5$, and $C_{21} = 1$, under two reflective modes. The following two conditions are considered: 1) The absorption optical thickness of the first layer $\tau_{a1}(=\alpha_1 d_1 = 0.1)$ is kept constant, while the optical thickness $\tau_1(=\kappa_1 d_1)$ is relatively increased from 0.1 in Fig. 6a to 10 in Fig. 6b with the scattering albedo ω_1 increased from 0 to 0.99. 2) Optical thickness $\tau_1(=0.1)$ is kept constant, while τ_{a1} is decreased from 0.1 (Fig. 6a) to 0.001 (Fig. 6c) with ω_1 increased from 0 to 0.99.

For case 1, the peak value of the temperature moves to the first layer throughout the transient time with the increase of the scattering albedo. When $\omega_1 = 0.99$, all of the peak values appear in the first layer, and the temperatures in the second layer lower greatly at the same time (Fig. 6b). This is because the same τ_{a1} and the larger ω_1 shield the second layer from incident radiation.

For case 2, the peak values of the temperature throughout the transient time appear in the second layer and near the internal interface (Fig. 6c). For the case of Fig. 6a, the effect of the reflective mode on the temperature field is larger than that for the other conditions because τ_{a1} is small (0.1) and without scattering. With the increase of ω_1, the effect of the reflective mode on the temperature field gets

Table 3 Dimensionless transient total heat flux densities $\tilde{q}^t$ at dimensionless coordinate $X = 0.9$

	Fig. 6a		Fig. 6b		Fig. 6c		Fig. 7	
t^*	Diffuse	Specular	Diffuse	Specular	Diffuse	Specular	Diffuse	Specular
0.1	1.1016	1.1682	0.4928	0.5232	1.2778	1.3124	0.4719	0.5019
0.4	1.5833	1.6170	0.5454	0.5784	1.8091	1.8320	0.5287	0.5602
t_s^*	1.8892	1.9090	0.7598	0.7945	1.9704	1.9946	0.7671	0.8008

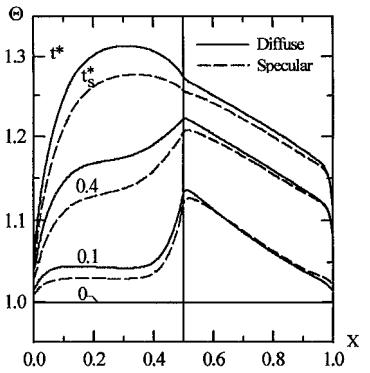

a) $\omega_1 = 0$, $\tau_1 = 0.1$; $\omega_2 = 0$, $\tau_2 = 5$

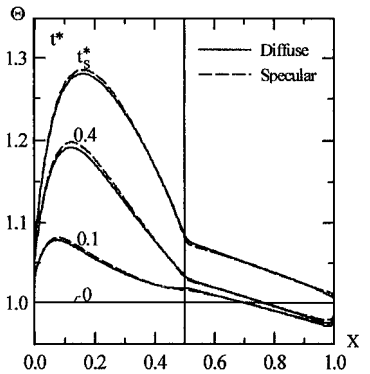

b) $\omega_1 = 0.99$, $\tau_1 = 10$; $\omega_2 = 0$, $\tau_2 = 5$

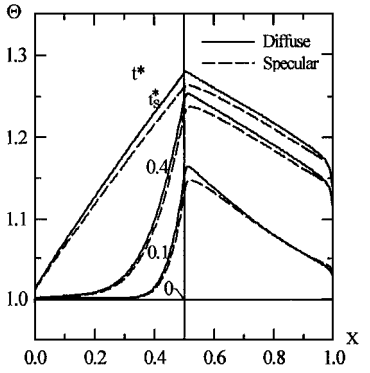

c) $\omega_1 = 0.99$, $\tau_1 = 0.1$; $\omega_2 = 0$, $\tau_2 = 5$

Fig. 6 Effect of ω_1 on temperature distributions.

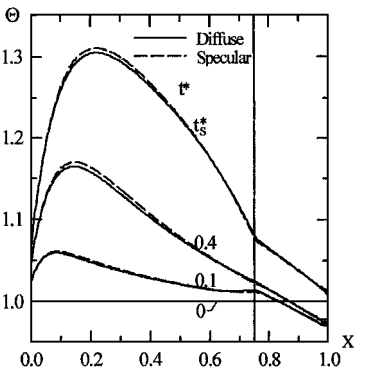

Fig. 7 Effect of δ_1 on temperature distributions.

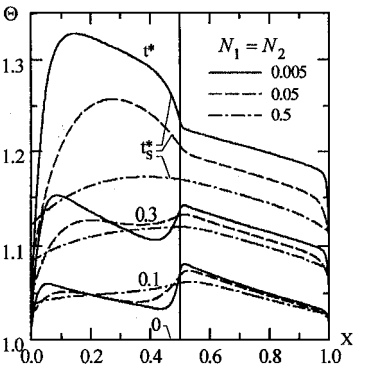

a) Diffuse reflection

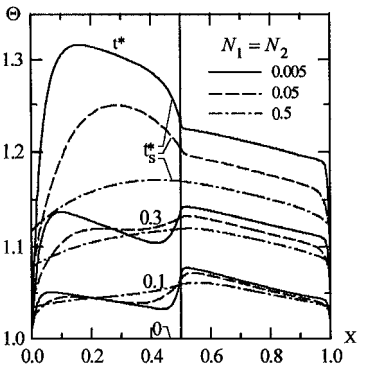

b) Specular reflection

Fig. 8 Effect of conduction–radiation parameter on temperature distributions.

small whether τ_{a1} or τ_1 is changed or not (Figs. 6b and 6c) because the isotropic scattering changes the direction of the ray transfer under specular reflection so that the transfer process is similar to that under diffuse reflection. The dimensionless total heat flux densities $\tilde{q}^t$ at the dimensionless coordinate $X = 0.9$ are shown in Table 3.

Effect of Dimensionless Thickness on Temperature Distributions

When $\delta = 0.5$, the two layers have equal thickness. Figure 7 shows the temperature distributions when the parameters are the same as those in Fig. 6b with the exception that $\delta = 0.75$, that is, $L_1 = 3L_2$. As shown in Figs. 7 and 6b, the general trend of temperature distributions is similar for both cases. The dimensionless total heat flux densities $\tilde{q}^t$ are also similar (Table 3).

Effect of the Conduction–Radiation Parameter on Temperature Distributions

The effect of the conduction–radiation parameter on the temperature distributions is shown in Fig. 8 for the case $n_1 = 1.5$, $n_2 = 3.0$, $\tau_1 = 1$, $\tau_2 = 2$, $\tilde{q}_{r1} = 1.5^4$, $\tilde{q}_{r2} = 0.5^4$, $H_1 = H_2 = 5$, $\tilde{T}_{g1} = \tilde{T}_{g2} = 1$, $\delta = 0.5$, $C_{21} = 1$, $\omega_1 = 0.9$, and $\omega_2 = 0$. The conduction–radiation parameter is changed from 0.005 (solid lines) to 0.05 (dotted lines) and 0.5 (dot–dash lines). Figure 8 shows the following: 1) With the decrease of the conduction–radiation parameter, the temperature gradient in the first layer becomes larger, and the temperature in the second layer is somewhat raised. 2) The general trends of temperature distributions are still similar for specular and diffuse reflection.

Effect of the Convection–Radiation Parameter on Temperature Distributions

When considering transient coupled radiative–conductive heat transfer, the conduction happens only in the adjoining region, but the radiation can take place over all of the semitransparent and transparent paths with relation to the optical thickness. Thus, if only the conduction is considered and there is no internal heat source, external energy can only transfer from the boundary surfaces to the inner part of the medium so that the temperatures decrease along the thickness. When the radiation is considered, at the moment and place when and where the accumulated energy becomes maximum, the temperature peak would appear. According to the preceding analysis, it is impossible for the temperature peak to appear in the opaque medium or in the semitransparent homogeneous medium with opaque boundary surfaces because the radiative energy cannot directly transfer to the inner part of the medium, but can only transfer to the inner part from the heated boundary surfaces by radiation and conduction.

In Ref. 22 it is pointed out that the main cause of the temperature peak appearing is the effect of radiation for the coupled radiative–conductive heat transfer in the homogeneous STM. Also, the following four conditions must be met at the same time (see Figs. 6–8): 1) The medium is semitransparent. 2) The boundary surfaces are semitransparent. 3) The semitransparent medium is subjected to external radiation. 4) The heated side is cooled by convection.

For an inhomogeneous medium, if the absorption coefficient in the inner part is higher than that in the part close to the surface, then the radiative energy absorbed in the inner part can be greater than that in the part close to the surface, though the surface is not cooled by convection. In this case, would there be a temperature peak in the STM ?

When the two layers of the semitransparent media have different physical properties, they can be considered as a single-layer inhomogeneous semitransparent medium. Under diffuse reflection, the temperature distributions for the composite without convection ($H_1 = H_2 = 0$) at boundary surfaces are given in Fig. 9 for the case $\tau_1 = 0.2$, $\tau_2 = 2$, $\tilde{q}_{r1} = 1.5^4$, $\tilde{q}_{r2} = 0.5^4$, $\delta = 0.5$, $C_{21} = 1$, $\omega_1 = 0.5$,

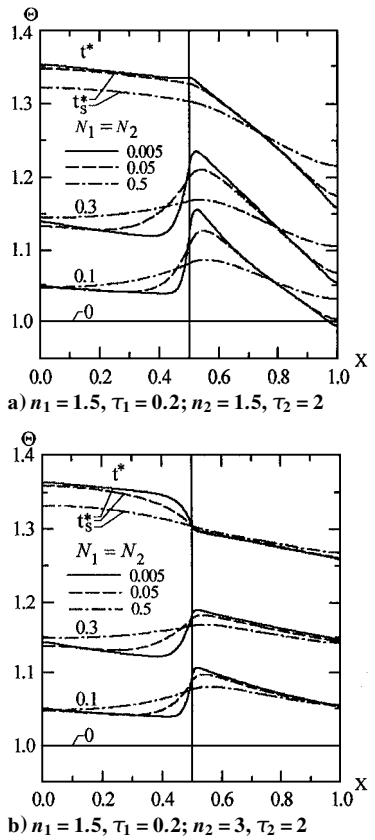

Fig. 9 Temperature distributions without convection ($H_1 = H_2 = 0$) at both boundaries.

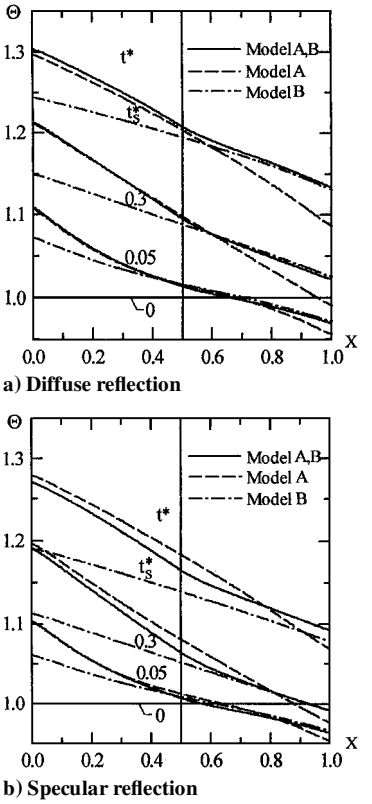

Fig. 10 Effect of the spectral band model on temperature distributions.

and $\omega_2 = 0.5$. As shown in Fig. 9, when the absorption coefficient of the second layer is larger than that of the first layer, the radiative energy absorbed by the second layer is greater than that by the first layer, so that, for the small t^*, the peak value or the maximum of temperature would appear within the media although there is no convective cooling on the surface. With the decrease of n_2 and N, the peak value or the maximum of temperature will become more obvious.

Effect of the Spectral Properties on Temperature Distributions

All of the preceding results are for the gray medium. Some results are given now for spectral band models A and B, as shown in Table 1, where both models have three spectral bands. The parameters are $\tilde{q}_{r1} = 1.5^4$, $\tilde{q}_{r2} = 0.5^4$, $N_1 = N_2 = 1.25$, $H_1 = H_2 = 1$, $\tilde{T}_{g1} = 1.5$, $\tilde{T}_{g2} = 0.5$, $\delta = 0.5$, and $C_{21} = 1$, where $L_1 = L_2 = 0.01$ m. Results, under the following three conditions, are given in Fig. 10: 1) Spectral band models A and B are applied to the first and the second layers, respectively (solid lines). 2) Both layers use model A (dashed lines). 3) Both layers use model B (dot–dash lines). Generally, the solid curve is similar to the dashed curve in the first layer and the dot–dash curve in the second layer. However, because the medium described by model A has isotropic scattering and strong absorption ability, for case 1, the effect of model A on the temperature distributions is more important than that of model B. When both layers use the same model, the temperature distributions for model B are more uniform than those for model A because the refractive index of the former is larger than that of the latter. For model B with the larger refractive index and without scattering, the effect of the reflective mode on the temperature distributions is larger than that of the model A. Therefore, the temperatures under diffuse reflection are higher than those under specular reflection for model B, but the trend of the temperature distributions is similar.

Radiative heat transfer is related to the space position, the spectral properties, and the space direction. Generally, the space zone is always dispersed in the calculation. The spectral properties are simulated by the three methods: the hypothesis of a gray medium, the average equivalent weight parameter method, and the spectral band model; the solid angle is also dispersed for most methods except for the zonal method, finite element method, and Monte Carlo methods,

such as the heat flux method,[17] the discrete transfer method,[23] the discrete intensity method,[24] the $P-N$ method,[25] the discrete ordinates method,[26] etc. For the single-layer absorbing, emitting, and isotropic scattering STM with specular reflection interfaces,[20] the method here has been verified by a comparison with the results in Refs. 27–29.

Conclusions

In this paper, under diffuse and specular reflection, respectively, the RTCs for a two-layer absorbing, emitting, and isotropic scattering semitransparent composite with both boundary surfaces semitransparent are derived using the ray tracing method and Hottel and Sarofim's zonal method.[21] The radiative heat source term is calculated by the RTCs. The transient energy equation is solved by the control-volume method in combination with the spectral band model. The transient temperature distributions and the heat flux densities in a composite layer are obtained for the general boundary conditions of external radiation and convection. The method developed here does not need to disperse the solid angle, but integrates it directly.

Under diffuse reflection, the temperature distributions are compared with an exact numerical solution[15] and an approximate solution[16] using Green's function and the two-flux method. The dimensionless heat flux densities are compared with those in Ref. 12. Comparison with results in Refs. 12, 15, and 16 verifies that the obtained RTC and the method adopted in this paper are correct. The method without discrete a solid angle is more accurate.

Illustrative results are provided to demonstrate the effects of the reflective mode, the scattering albedo, the dimensionless thickness, the conduction–radiation parameter, the convection–radiation parameter, and the spectra properties on temperature distributions and heat flux densities. Thereby, the following conclusions can be obtained:

1) When the absorption coefficient of a composite layer is small and without scattering, the reflective mode of the surface has a greater effect on the temperatures.

2) Increasing the scattering albedo can reduce the difference of the temperature distributions caused by reflective mode, so that the difference caused by reflective mode can be negligible for the media with intense isotropic scattering.

3) For inhomogeneous media (two-layer semitransparent media with different physical properties can be considered as a single-layer inhomogeneous semitransparent medium), the radiative energy absorbed by the control-volume with a large absorption coefficient is greater than that absorbed by the control-volume with a small absorption coefficient. With this condition, although there is no convective cooling on the surface, the peak value or maximum of the transient temperature may nevertheless appear inside the media.

Appendix: RTC and Its Relativity Under Diffuse Reflection

RTC for an Absorbing, Emitting Composite

For the direct exchange area,

$$(s_b s_P)_k = 2\int_0^1 \exp(-\kappa_{b,k} L_b/\mu)\mu \, \mathrm{d}\mu \tag{A1}$$

$$(s_c v_{b_j})_k = 2\int_0^1 \left\{\exp(-\kappa_{b,k} x_{c,b_h}/\mu) - \exp\left[-\kappa_{b,k}(x_{c,b_h} + \Delta x)/\mu\right]\right\}\mu \, \mathrm{d}\mu \tag{A2}$$

$$(v_{b_i} v_{b_j})_k = 2\int_0^1 \left\{\exp(-\kappa_{b,k} x_{b_{i+1},b_j}/\mu) - 2\exp(-\kappa_{b,k} x_{b_i,b_j}/\mu) + \exp(-\kappa_{b,k} x_{b_i,b_{j+1}}/\mu)\right\}\mu \, \mathrm{d}\mu \quad (i \neq j) \tag{A3}$$

$$(v_{b_i} v_{b_j})_k = 4\kappa_{b,k}\Delta x - 2[1 - 2E_3(\kappa_{b,k}\Delta x)] \quad (i = j) \tag{A4}$$

where if $b = 1$ and $c = P$, or $b = 2$ and $c = 2$, then $h = j + 1$, otherwise, $h = j$.

For convenience, two functions are defined:

$$FM_{b,k} = \rho_{bP}\rho_{bg}(s_b s_P)_k^2 \tag{A5}$$

$$FM_k = \frac{\gamma_{1P}\gamma_{2P}\rho_{1g}\rho_{2g}(s_1 s_P)_k^2 (s_2 s_P)_k^2}{(1 - FM_{1,k})(1 - FM_{2,k})} \tag{A6}$$

For $FM_{b,k}$, under diffuse reflection, the total radiative energy reaching some element is a geometric progression in the transferring process of the radiative intensity in the single-layer (bth layer) STM. $FM_{b,k}$ is the common ratio. For FM_k, the total radiative energy absorbed by some element is also a geometric progression in the transfer process of the radiative intensity in the two-layer STM. FM_k is the common ratio.

For the expressions of RTC,

$$(S_u S_u)_k^d = \rho_{gb} + \frac{\gamma_{gb}\gamma_{bg}\rho_{bP}(s_b s_P)_k^2}{1 - FM_{b,k}} + \frac{\gamma_{gb}\gamma_{bP}\rho_{cg}\gamma_{cP}\gamma_{bg}(s_c s_P)_k^2 (s_b s_P)_k^2}{(1 - FM_{1,k})(1 - FM_{2,k})(1 - FM_k)(1 - FM_{b,k})} \tag{A7}$$

$$(S_u V_{b_j})_k^d = \frac{(s_b v_{b_j})_k + \rho_{bP}(s_b s_P)_k (s_P v_{b_j})_k}{(1 - FM_{b,k})/\gamma_{gb}} + \frac{\gamma_{bP}\rho_{cg}\gamma_{cP}(s_b s_P)_k (s_c s_P)_k^2 \left[(s_P v_{b_j})_k + (s_b s_P)_k \rho_{bg}(s_b v_{b_j})_k\right]}{(1 - FM_{1,k})(1 - FM_{2,k})(1 - FM_k)(1 - FM_{b,k})/\gamma_{gb}} \tag{A8}$$

$$(S_u V_{c_j})_k^d = \frac{\gamma_{gb}\gamma_{bP}(s_b s_P)_k \left[(s_P v_{c_j})_k + (s_c s_P)_k \rho_{cg}(s_c v_{c_j})_k\right]}{(1 - FM_{1,k})(1 - FM_{2,k})(1 - FM_k)} \tag{A9}$$

In Eqs. (A7–A9), if $u = -\infty$, then $b = 1$ and $c = 2$; otherwise $b = 2$ and $c = 1$.

$$(V_{b_i} V_{b_j})_k^d = (v_{b_i} v_{b_j})_k + \frac{(s_b v_{b_i})_k \rho_{bg}\left[(s_b v_{b_j})_k + (s_b s_P)_k \rho_{bP}(s_P v_{b_j})_k\right]}{1 - FM_{b,k}} + \frac{(s_P v_{b_i})_k \rho_{bP}\left[(s_P v_{b_j})_k + (s_b s_P)_k \rho_{bg}(s_b v_{b_j})_k\right]}{1 - FM_{b,k}} + \frac{\left[(s_b v_{b_i})_k \rho_{bg}(s_b s_P)_k \gamma_{bP} + (s_P v_{b_i})_k \gamma_{bP}\right]\rho_{cg}\gamma_{cP}(s_c s_P)_k^2 \left[(s_P v_{b_j})_k + (s_b s_P)_k \rho_{bg}(s_b v_{b_j})_k\right]}{(1 - FM_{1,k})(1 - FM_{2,k})(1 - FM_k)(1 - FM_{b,k})} \tag{A10}$$

In Eq. (A10), if $b = 1$, then $c = 2$, otherwise $c = 1$.

$$(V_{1_i} V_{2_j})_k^d = \frac{\gamma_{1P}\left[(s_1 v_{1_i})_k \rho_{1g}(s_1 s_P)_k + (s_P v_{1_i})_k\right] \times \left[(s_P v_{2_j})_k + (s_2 s_P)_k \rho_{2g}(s_2 v_{2_j})_k\right]}{(1 - FM_{1,k})(1 - FM_{2,k})(1 - FM_k)} \tag{A11}$$

Relativity of RTC

For diffuse reflection, the total reflection is considered in the reflectivity and transmissivity, so that the transmissivity and reflectivity of different sides of an interface are different. The relativities of the RTCs are

$$
\begin{aligned}
(S_{-\infty}\, S_{+\infty})_k^d \gamma_{g2}\gamma_{2P}\gamma_{1g} &= (S_{+\infty}\, S_{-\infty})_k^d \gamma_{g1}\gamma_{1P}\gamma_{2g} \\
(S_{-\infty}\, V_{1_j})_k^d \gamma_{1g} &= (V_{1_j}\, S_{-\infty})_k^d \gamma_{g1} \\
(S_{-\infty}\, V_{2_j})_k^d \gamma_{2P}\gamma_{1g} &= (V_{2_j}\, S_{-\infty})_k^d \gamma_{1P}\gamma_{g1} \\
(S_{+\infty}\, V_{1_j})_k^d \gamma_{1P}\gamma_{2g} &= (V_{1_j}\, S_{+\infty})_k^d \gamma_{2P}\gamma_{g2} \\
(S_{+\infty}\, V_{2_j})_k^d \gamma_{2g} &= (V_{2_j}\, S_{+\infty})_k^d \gamma_{g2} \\
(V_{1_i}\, V_{2_j})_k^d \gamma_{2P} &= (V_{2_j}\, V_{1_i})_k^d \gamma_{1P} \\
(V_{1_i}\, V_{1_j})_k^d = (V_{1_j}\, V_{1_i})_k^d, &\qquad (V_{2_i}\, V_{2_j})_k^d = (V_{2_j}\, V_{2_i})_k^d \qquad \text{(A12)}
\end{aligned}
$$

Acknowledgments

This research is supported by the Chinese National Science Fund for Distinguished Young Scholars (Number 59725617) and the National Natural Science Foundation of China (Number 59606006).

References

[1]Kunc, T., Lallemand, M., and Saulnier, J. B., "Some New Developments on Coupled Radiative-Conductive Heat Transfer in Glasses–Experiments and Modelling," *International Journal of Heat and Mass Transfer*, Vol. 27, No. 12, 1984, pp. 2307–2319.

[2]Field, R. E., and Viskanta, R., "Measurement and Prediction of the Dynamic Temperature Distributions in Soda Lime Glass Plates," *Journal of the American Ceramic Society*, Vol. 73, No. 7, 1990, pp. 2047–2053.

[3]Ducharme, R., Kapadia, P., Scarfe, F., and Dowden, J., "A Mathematical-Model of Glass Flow and Heat-Transfer in a Platinum Downspout," *International Journal of Heat and Mass Transfer*, Vol. 36, No. 7, 1993, pp. 1789–1797.

[4]Thomas, J. R., Jr., "Coupled Radiation/Conduction Heat Transfer in Ceramic Liners for Diesel Engines," *Numerical Heat Transfer*, Pt. A, Vol. 21, No. 1, 1992, pp. 109–120.

[5]Song, B., and Viskanta, R., "Deicing of Solids Using Radiant Heating," *Journal of Thermophysics and Heat Transfer*, Vol. 4, No. 3, 1990, pp. 311–317.

[6]Howe, J. T., and Yang, L., "Earth Atmosphere Entry Thermal Protection by Radiation Backscattering Ablating Materials," *Journal of Thermophysics and Heat Transfer*, Vol. 7, No. 1, 1993, pp. 74–81.

[7]Cornelison, C. J., and Howe, J. T., "Analytic Solution of the Transient Behavior of Radiation Backscattering Heat Shields," *Journal of Thermophysics and Heat Transfer*, Vol. 6, No. 4, 1992, pp. 612–617.

[8]Chan, S. H., and Cho, D. H., "Transient Radiative Heat Transfer Between Two Emitting–Absorbing Media," *Proceedings of the 6th International Heat Transfer Conference*, Vol. 31, Hemisphere, Washington, DC, 1978, pp. 367–372.

[9]Tsai, C. F., and Nixon, G., "Transient Temperature Distribution of a Multilayer Composite Wall with Effects of Internal Thermal Radiation and Conduction," *Numerical Heat Transfer*, Vol. 10, No. 1, 1986, pp. 95–101.

[10]Timoshenko, V. P., and Trenev, M. G., "A Method for Evaluation Heat Transfer in Multilayer Semitransparent Materials," *Heat Transfer–Soviet Research*, Vol. 18, No. 5, 1986, pp. 44–57.

[11]Ho, C. H., and Özisik, M. N., "Combined Conduction and Radiation in a Two-Layer Planar Medium with Flux Boundary Condition," *Numerical Heat Transfer*, Vol. 11, No. 3, 1987, pp. 321–340.

[12]Siegel, R., and Spuckler, C. M., "Refractive Index Effects on Radiation in an Absorbing, Emitting, and Scattering Laminated Layer," *Journal of Heat Transfer*, Vol. 115, No. 1, 1993, pp. 194–200.

[13]Siegel, R., and Spuckler, C. M., "Variable Refractive Index Effects on Radiation in Semitransparent Scattering Multilayered Regions," *Journal of Thermophysics and Heat Transfer*, Vol. 7, No. 4, 1993, pp. 624–630.

[14]Siegel, R., and Spuckler, C. M., "Approximate Solution Methods for Spectral Radiative Transfer in High Refractive Index Layers," *International Journal of Heat and Mass Transfer*, Vol. 37, Supplement 1, 1994, pp. 403–413.

[15]Spuckler, C. M., and Siegel, R., "Refractive Index and Scattering Effects on Radiation in a Semitransparent Laminated Layer," *Journal of Thermophysics and Heat Transfer*, Vol. 8, No. 2, 1994, pp. 193–201.

[16]Siegel, R., "Green's Function and Two-Flux Analysis for Transient Radiative Transfer in a Composite Layer," *Proceedings of the National Heat Transfer Conference*, Vol. 325, American Society of Mechanical Engineers, Fairfield, NJ, 1996, pp. 35–43.

[17]Siegel, R., "Temperature Distribution in a Composite of Opaque and Semitransparent Spectral Layers," *Journal of Thermophysics and Heat Transfer*, Vol. 11, No. 4, 1997, pp. 533–539.

[18]Siegel, R., "Transient Thermal Effects of Radiant Energy in Translucent Materials," *Journal of Heat Transfer*, Vol. 120, No. 1, 1998, pp. 4–23.

[19]Tan, H. P., and Lallemand, M., "Transient Radiative-Conductive Heat Transfer in Flat Glasses Submitted to Temperature, Flux and Mixed Boundary Conditions," *International Journal of Heat and Mass Transfer*, Vol. 32, No. 5, 1989, pp. 795–810.

[20]Tan, H. P., Ruan, L. M., Xia, X. L., Yu, Q. Z., and Tong, T. W., "Transient Coupled Radiative and Conductive Heat Transfer in an Absorbing, Emitting, and Scattering Medium," *International Journal of Heat and Mass Transfer*, Vol. 42, No. 15, 1999, pp. 2967–2980.

[21]Hottel, H. C., and Sarofim, A. F., *Radiative Transfer*, McGraw–Hill, New York, 1967, pp. 265, 266.

[22]Tan, H. P., Yu, Q. Z., and Tong, T. W., "Numerical Analysis of Temperature Field in Materials During Infrared Heating," *Chinese Journal of Infrared and Millimeter Waves*, Vol. 10, No. 2, 1991, pp. 169–178.

[23]Lockwood, F. C., and Shah, N. G., "A New Radiation Solution Method for Incorporation in General Combustion Prediction Procedures," *Eighteenth Symposium (International) on Combustion*, Combustion Inst., Pittsburgh, PA, 1981, pp. 1405–1414.

[24]Shih, T. M., and Chen, Y. N., "A Discretized Intensity Method Proposed for Two Dimensional Systems Enclosing Radiative and Conductive Media," *Numerical Heat Transfer*, Vol. 6, No. 2, 1983, pp. 117–134.

[25]Ratzel, A. C., and Howell, J. R., "Two Dimensional Radiation in Absorbing Emitting Media Using the P–N approximation," *Journal of Heat Transfer*, Vol. 105, No. 2, 1983, pp. 333–340.

[26]Fiveland, W. A., "Discrete Oradinates Solutions of the Radiative Transport Equation for Rectangular Enclosures," *Journal of Heat Transfer*, Vol. 106, No. 4, 1984, pp. 699–706.

[27]Siegel, R., "Separation of Variables Solution for Non-Linear Radiative Cooling," *International Journal of Heat and Mass Transfer*, Vol. 30, No. 5, 1987, pp. 959–965.

[28]Machali, H. F., and Madkour, M. A., "Radiative Transfer in a Participating Slab with Anisotropic Scattering and General Boundary Conditions," *Journal of Quantitative Spectroscopy and Radiative Transfer*, Vol. 54, No. 5, 1995, pp. 803–813.

[29]Frankel, J. I., "Cumulative Variable Formulation for Transient Conductive and Radiative Transport in Participating Medium," *Journal of Thermophysics and Heat Transfer*, Vol. 9, No. 2, 1995, pp. 210–218.